Measurement of the electrical resistivity of hot aluminum passing from the liquid to gaseous state at supercritical pressure

V. N. Korobenko, A. D. Rakhel,* A. I. Savvatimski, and V. E. Fortov
Institute for High Energy Densities, Izhorskaya 13/19, Moscow 125412, Russia
(Received 17 August 2004; published 25 January 2005)

Thin aluminum foil strips tamped by polished glass plates were rapidly heated by means of a pulse current. The experimental technique has ensured a sufficiently homogeneous heating of the foil samples during continuous expansion from the liquid to gaseous state at a pressure of 7–60 kbar. Results on the electrical resistivity of aluminum were obtained in a density range extending from about the normal solid density down to a density 30 times less and in a temperature range from 6000 to 50 000 K. A dielectriclike dependence of the resistivity on temperature along isochore was observed at a density, which is 4 times less than the normal solid density. A maximum in the temperature dependence of the resistivity was detected along an isochore corresponding to a density that is 5.4 times less than the normal solid density. Present results confirm recent theoretical predictions based on finite-temperature density-functional theory about the behavior of the electrical resistivity of aluminum in the liquid and gaseous state.

DOI: 10.1103/PhysRevB.71.014208 PACS number(s): 72.15.Cz, 71.30.+h, 52.25.−b, 52.70.−m

I. INTRODUCTION

Much work has been done in the last decade in the exploration of thermodynamic and transport properties of liquid metals, the density of which has been significantly lowered (say, with respect to the triple point density). These studies were focused mainly on two general problems: a description of the metal-nonmetal transition occurring in such systems[1–4] and the dense metallic plasmas characterized by strong interparticle interaction (strongly coupled plasmas).[5–8] There is also a practical interest in studying such states of matter caused by some pulse-powered applications, in which a metallic sample is rapidly heated so that due to inertia its density remains relatively high despite a considerable rise in temperature. Phenomena such as electron band crossings, electron shell ionization, and phase transitions all may occur in the hot dense matter generated under these conditions.[5]

A theoretical description of expanded metals and dense metallic plasmas presents a complicated problem that is still not well understood. Recently several theoretical papers have been published, in which the electrical conductivity and thermodynamic functions of aluminum were calculated in wide domains of temperature and density including condensed and gaseous states as well.[9–12] To validate the calculations the corresponding experimental studies are highly desired.

The available experimental data on expanded metals are restricted to relatively low temperatures and pressures. In the case of aluminum $T<4000$ K, and $P\leqslant 3$ kbar,[13] which correspond to a narrow density range of 2.7–1.8 g/cm^3. Only some alkali metals and mercury have sufficiently low critical points to be studied by means of a steady-state technique in the so-called metal-nonmetal transition region, i.e., during a continuous expansion from the liquid to gaseous state without crossing the liquid-vapor equilibrium line. To study metals with higher critical points (for example, aluminum) dynamic methods should be utilized.[5]

The most extensive data at the higher temperatures and pressures were obtained in the experiments on exploding wires[8,14,15] and foils.[10,11] The main goal of those studies was to measure the electrical conductivity of dense plasmas. To perform the measurements at sufficiently high densities different confinement media were used (lead-glass,[8] silica glass,[14] and water[15]). In those experiments the electrical conductivity was determined assuming the temperature, pressure, and other quantities are distributed uniformly over the plasma. Shadow images of the plasma column formed by an exploding wire demonstrated in some experiments its axial symmetry and uniformity along the length. However, efforts to control the radial distributions of the quantities were unsuccessful. In all experiments mentioned above at the initial stage of the heating process the dynamic pressure generated was not sufficiently high to prevent the liquid-vapor phase transition. Volume vaporization (boiling) at the heating rates utilized in those measurements leads to nonuniform temperature and pressure distributions in the expanding column due to a large difference between the sound speeds and resistivities of a liquid and that of the two-phase liquid-gas mixture.[16] Therefore the question about the uncertainty of the measurements[8,10,14,15] remains unanswered.

In present work we use the experimental technique[17,18] that ensures a highly homogeneous heating of metallic samples during continuous changing from a condensed into a gaseous state. Thin metallic foils tamped by relatively thick silica glass or sapphire plates are heated by an intense current pulse so that the dynamic pressure generated is sufficiently high to prevent the liquid-vapor phase transition. As a result, uniform, sufficiently long-lived ($\geqslant$100 ns) single-phase states are produced, which are amenable to comprehensive diagnostics and simulation. Earlier,[18] we reported the results of experiments utilizing this technique to measure the electrical conductivity of mercury in the metal-nonmetal transition region. Comparison of the data obtained in those experiments with steady-state measurements[1] has shown a fairly good agreement, justifying that the developed dynamic technique is capable of performing sufficiently accurate measurements.

In this paper the dependence of the aluminum resistivity on the temperature and density is reported in a density range

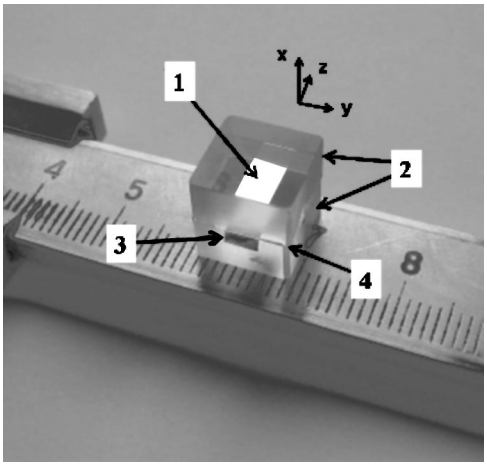

FIG. 1. Photograph of an aluminum foil strip (1) confined by two polished silica glass plates (2). The sample ends (3) were bent and pressed to the electrodes delivering the current pulse. The gap (4) between the glass plates was filled with epoxy. The foil strip shown has a thickness of 9 μm, a width of 3 mm, and a length of about 10 mm.

extending from about the normal solid density down to a density 20 to 30 times less and in a temperature range from about 6000 up to 50 000 K. We compare the data obtained with the published experimental results[8,10,14,15] and discuss the cause of the discrepancies observed. Comparison of present results with those of the calculations[7,9–12] has shown good agreement, but only with the results of the molecular dynamics simulations based on finite-temperature density-functional theory.[9,12]

This paper is organized as follows. In Sec. II we present in detail the experimental technique utilized. This technique does not allow us to measure directly all the quantities, which are necessary to determine the electrical resistivity and to characterize completely thermodynamic state of the sample. Some quantities are calculated using a magnetohydrodynamic (MHD) code and an equation of state model of aluminum. In Sec. III the equation of state models used are described. The procedure of the MHD calculations is presented in Sec. IV. The main results on the electrical resistivity of aluminum are given in Sec. V. Comparison of present data with the literature data is discussed in Sec. VI. Conclusions are presented in Sec. VII.

II. EXPERIMENTAL SETUP AND DESCRIPTION OF THE APPROACH

The experiments were carried out with aluminum foil strips, with a thickness (d) of 9 to 16.5 μm, a width (h) of 1.5 to 3 mm, and a length (l) of about 10 mm. A foil sample was placed between two polished (of mirror quality) sapphire or silica glass plates having a thickness of 3 to 5 mm, a width of 10 mm, and a length of about 10 mm (see Fig. 1). The experimental assembly was made in such a way that there were no gaps between the sample and the plates. High quality tamping is ensured by epoxy glue, completely filling the space between the aluminum foil and the glass plates. As a result, the positions of the plates with the foil strip pressed between were fixed precisely. An optical microscope examination was used to check the quality of the assembly.

Geometrical dimensions of the experimental assembly were chosen such that a one-dimensional expansion of the sample is realized, i.e., the sample material moves along the x axis mainly (see Fig. 1); we introduced a Cartesian coordinate system, the x axis of which is directed perpendicular to the foil strip surface and the z axis along the heating current. The reason for the one-dimensional expansion is the following. For a foil strip whose dimensions satisfy the inequalities $l \gg h \gg d$ (as was the case for all our experiments) the acoustic time corresponding to the sample thickness d/c_1 (c_1 is the sound speed of the sample material) is much smaller than those corresponding to the sample width and length. In this case the pressure gradient in the bulk of the sample is directed along the x axis and therefore the sample material moves in this direction. At the same time one should keep in mind that the boundary conditions at the foil strip edges differ only slightly from those at the front surface far from the edges (there are no gaps between the sample and the glass plates); therefore the displacement of the sample material along the y axis at the sample edges is of the same order of the magnitude as that at the sample front surface far from the edges in the x direction. It should be noted that in order to produce the one-dimensional (1D) expansion the pressure wave formed in the glass plates should be rather flat. In our experiments it is ensured by an appropriate temporal dependence of the Joule heating power, which causes glass acceleration during a sufficiently short time with respect to the acoustic time h/c_2 (c_2 is the longitudinal speed of sound in glass).

The pulse heating of the foil samples was accomplished by discharging a 72-μF capacitor bank at a charging voltage of 5 to 24 kV. Schematics of the electrical circuit producing the current pulse, the aluminum foil confined by two glass plates, and the diagnostics used are depicted in Fig. 2.

Diagnostics in these experiments were the following. The voltage across the foil strip was measured by means of a resistive divider, and the current through it by a Rogowski coil. All electrical waveforms were recorded with a four-channel, 1-GHz sample rate digital oscilloscope, Tektronix TDS 754C. The resistance of the sample R and the specific Joule heat dissipated in it q as functions of time were determined from the measured quantities by

$$R = U_R/I, \tag{1}$$

$$q = \int_0^t IU_R dt'/M, \tag{2}$$

where U_R is the resistive voltage contribution, I is the electrical current, M is the sample mass, and t is the time. The voltage U_R was calculated by subtracting from the measured voltage U an inductive voltage contribution

$$U_R = U - L_S dI/dt, \tag{3}$$

where L_S is the sample inductance. To get the sample inductance we measured the current and voltage waveforms for a

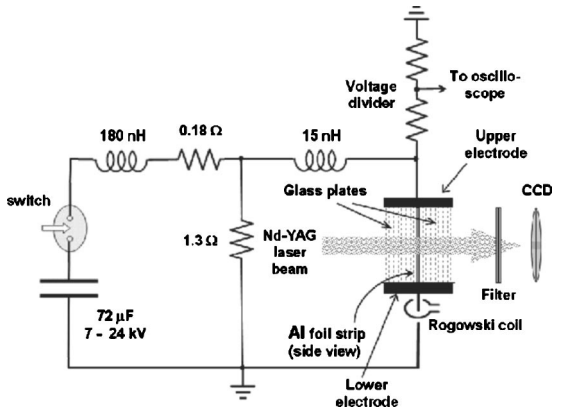

FIG. 2. Schematics of the electrical circuit producing the heating current pulse, the foil sample confined by two glass plates (side view), and the diagnostics used in these experiments. The current pulse was produced by discharging the capacitor bank in the circuit containing the foil sample, a ballast resistor (0.18 Ω) and a shunt resistor (1.3 Ω). A Nd:YAG laser pulse of 9 ns duration was used for high-speed optical photographing of the expanded foil strip to control the sample symmetry during the measurements.

shorted circuit, where a copper wire of 1 mm in diameter and 1 cm long was used in place of the sample.

To check that our current and voltage measurements were performed accurately we compared the dependence of the normalized resistance $R^*=RS_0/l$ (S_0 is the initial cross-sectional area of the foil strip and l is its length) on the specific Joule heat released with the literature data. For a homogeneously heated sample, the resistance so normalized is equal to the ratio of the resistivity σ^{-1} (σ is the conductivity) to the relative volume V/V_0, where V_0 is the specific volume of the sample material at normal conditions. In Fig. 3 the dependencies of the normalized resistance versus specific enthalpy measured in our experiments are compared with the data obtained by Gathers.[13] It can be easily seen that the specific Joule heat q practically coincides with the enthalpy in the enthalpy range, for which the data of Ref. 13 were obtained. As one can see there is a fairly good agreement between our results and those presented in Ref. 13 for an isobaric heating at $P=3$ kbar. The discrepancy seen at small

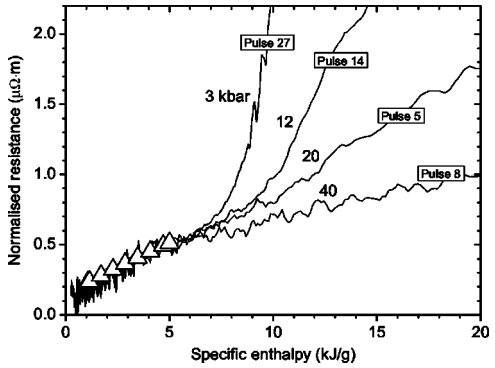

FIG. 3. Normalized resistance vs specific enthalpy: our data (lines), experiments on isobaric heating at $P=3$ kbar (Ref. 13) (open triangles). Pressures for our experiments are indicated for an enthalpy of 10 kJ/g.

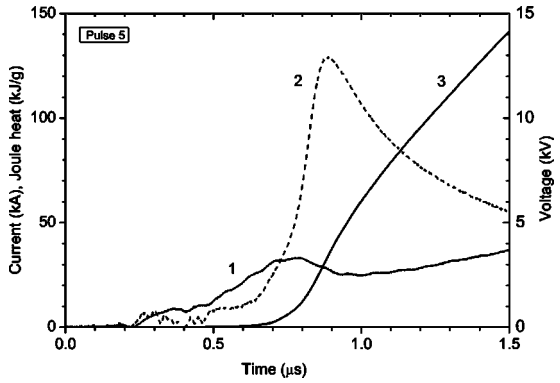

FIG. 4. Temporal dependencies of the current through the foil sample (1), the resistive voltage (2), and the specific Joule heat released (3). The foil strip sample had a thickness of 16.5 μm, a width of 3 mm, and a length of 10 mm (pulse 5).

enthalpies is due to the skin effect and a low signal to noise ratio in the current and voltage signals at the early beginning of the heating process in our measurements. Figure 3 demonstrates that our measurements are rather accurate and the resistive voltage contribution U_R was determined correctly. The dynamic pressures generated in our experiments at a value of the Joule heat of 10 kJ/g are also indicated in Fig. 3. The pressures were calculated using an equation of state model for aluminum and a one-dimensional hydrodynamic code describing the foil expansion. This point will be discussed in detail in Secs. III and IV.

The electrical conductivity was determined according to the formula

$$\sigma = \frac{l}{S(t)R}, \tag{4}$$

where $S(t)$ is the current cross-sectional area of the sample, i.e., the product of the sample width h and thickness $d(t)$. The thickness as a function of time was calculated using 1D MHD code assuming the sample length and width are constant.

Temporal dependencies of the current through the foil strip, the voltage drop across its length (the resistive part), and the Joule heat released in it measured in a typical experiment are shown in Fig. 4. As one can see, the heating power (the slope of the Joule heat dependence) changes considerably for about 100–200 ns and then remains nearly constant. Such temporal dependence is very important for realizing homogeneous heating of a sample, whose thickness increases significantly. The voltage curve shows a maximum, which manifests a transition of aluminum from a metallic to a dielectric state (plasma); as the current variations at later times ($t>600$ ns) become relatively small the resistance temporal dependence is similar to that of the resistive voltage. Hence, the resistance increases up to the Joule heat values of about 40 kJ/g that exceeds three times the cohesion energy of aluminum [12.1 kJ/g (Ref. 19)] and then at higher Joule heat values ($q>40$ kJ/g) it monotonically decreases like a plasma does with a rise in temperature.

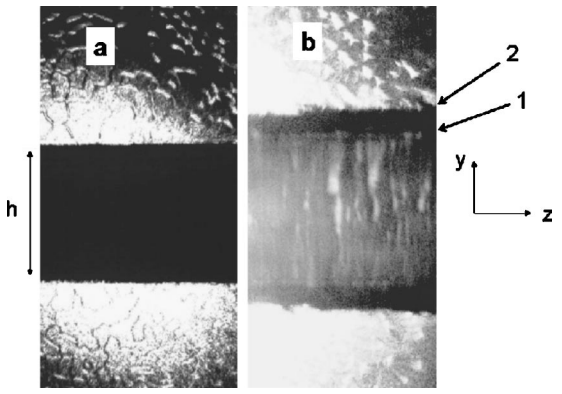

FIG. 5. Photograph of an Al foil strip confined between two polished silica glass plates (front view) before the current is switched on (a) and after a tenfold expansion in the x direction (b); electrical current flows in the z direction. The Joule heat released in the sample at the instant of time corresponding to photograph (b) reaches a value of 39 kJ/g. The initial width of the foil strip was 2.0 mm and the thickness of 16.5 μm. The arrows show the sample edge (1) and the failure wave front propagating in silica glass (2).

To prove that the sample symmetry during the measurements is kept and the bulk of the sample material moves along the x axis, high-speed optical photographing of the foil samples during the pulse heating process has been performed. A Nd:YAG (YAG denotes yttrium aluminum garnet) laser operated at the second harmonic ($\lambda = 532$ nm) with a pulse duration of 9 ns was used for the frame shadowgraphy. A laser beam propagating in the x direction formed a shadow image of the sample at the input of a CCD camera (see Fig. 2). Before reaching the CCD camera objective, the light was transmitted through a narrow-band interference filter (central wavelength of 532 nm, with a full width at half maximum of 1 nm). The frame images of the foil sample before the heating current is switched on (a) and after a tenfold expansion along the x axis (b) as it was predicted by 1D MHD calculations are shown in Fig. 5. It can be clearly seen that the sample edges after the tenfold expansion are still sufficiently straight. The displacement of the sample material along the y axis estimated from these images is within 100–200 μm, which is comparable to that in the x direction (the initial thickness of the foil was 16.5 μm). The nontransparent regions adjacent to the sample edges are due to the failure wave generated in silica glass, which was observed by Kanel *et al.*[20] The white spots on the sample area seen in photograph (b) are due to the light scattered from the optical interfaces of the experimental assembly.

In conclusion, in this section we present some estimates supporting the assumption of homogeneity of the foil samples during the measurements. The electric current pulse produced by the discharge circuit was chosen in such a way that the characteristic time t_j, for which the heating power increases (say, twofold) is considerably larger than the acoustic time d/c_1 (this time increases from about 1 ns when the sample is in the solid state to about 100 ns in a plasma state). As a result, the pressure profile (distribution as a function of position along the x axis) remains uniform. On the other hand, the acoustic time D/c_2 is much larger than the time t_j, where D is the glass plate thickness. The time during which the measurements are carried out is smaller than the time $2D/c_2$, for which the compression wave formed in a glass plate reaches its free surface and then a rarefaction wave arrives at the sample. This time is about 2 μs for the silica glass plates and 0.9 μs for sapphire plates (both having a thickness of 5 mm). Consequently, during this time the pressure in the sample remains high and the temperature and density profiles in the sample are not disturbed by the wave reflected from the free surface. It is easy to see that geometrical dimensions of the experimental assembly are such that the pressure wave propagating in the y direction also does not disturb the sample for the measurement time.

To ensure homogeneous heating the sample thickness was chosen to be smaller than the skin depth. It is easy to see also that the temperature gradient due to the thermal conduction is formed in a very thin layer of the glass plate close to the sample surface. Indeed, the thickness of the layer is of the order of $\sqrt{\chi_2 t_m}$, where χ_2 is the thermal diffusivity of glass and t_m is a typical time of the measurements. For a time $t_m \sim 1$ μs and for $\chi_2 \sim 0.01$ cm^2/s, this estimate gives a value of the order of 1 μm, which is much smaller than the thickness of an expanded sample (that is, within 200–300 μm). Therefore the energy losses and the wall ablation effect can be neglected. Estimates show that the energy losses due to the radiation should be taken into account at $T > 50\,000$ K when the sample density decreases 30–50 times. Another factor that can violate the pressure uniformity in the sample is the ponderomotive force (the pinch effect). In our experiments this pressure contribution was usually of the order of 0.1 kbar, which is a small value compared with the typical pressure level generated in present experiments.

III. THERMODYNAMIC FUNCTIONS OF ALUMINUM AND THE CONFINING MEDIA

As described in the preceding section we measure directly only two quantities: the resistance of the foil and the Joule heat released in it. The sample thickness and thermodynamic quantities (density, pressure, and temperature) were calculated using an equation of state model and the 1D MHD code utilized earlier.[16–18] Since the relevance of the 1D approach in the simulations is controlled by high-speed photography, the quality of present data on the electrical resistivity depends mainly on the quality of the equation of state (EOS) model used. In this work we utilized the SESAME EOS model [table no. 3720 (Ref. 21)] and the wide range semiempirical EOS model described in Refs. 16 and 22. The SESAME tables were used in many works devoted to the measurements of the electrical conductivity of dense aluminum plasmas,[8,10,14,15] and this was the main reason to use the tables in this work.

The analytical multiphase equation of state model of Ref. 22 was carefully analyzed in Ref. 16 for the region of the liquid-to-vapor phase transition (up to the critical point) in the case of tungsten. Thermodynamic functions of the EOS model in the condensed state were taken in the form proposed by Young.[23] Ionization effects were described in the average atom approximation.[24] It should be noted that the

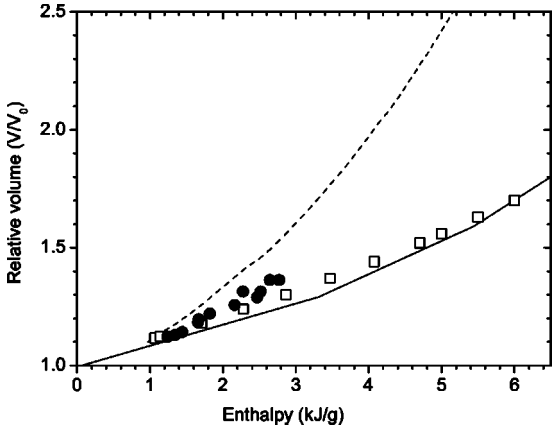

FIG. 6. Dependence of the relative volume of liquid aluminum vs enthalpy for an isobar $P=3$ kbar calculated using the EOS model from Ref. 22 (solid line), SESAME table 3720 (Ref. 21) (dashed line), measured in Ref. 13 (open squares) and measured in Ref. 25 (solid circles).

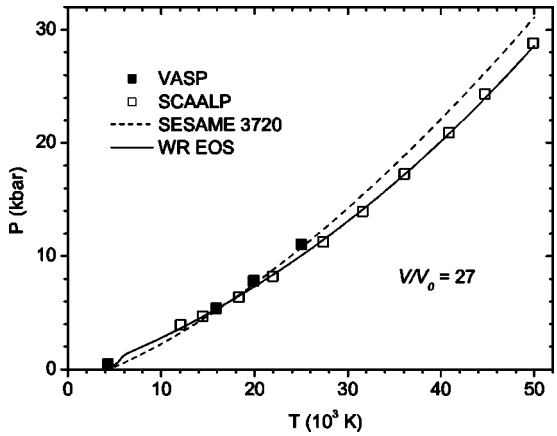

FIG. 7. Pressure as a function of temperature at constant density ($V/V_0=27$) calculated by means of the wide range EOS model (Ref. 22) (solid line), SESAME table 3720 (Ref. 21) (dashed line), calculation results of Ref. 11 (open squares), and calculated by the VASP code (Ref. 26) (solid squares). The points corresponding to VASP results were taken from Fig. 5 of Ref. 11.

average atom approximation cannot reproduce accurately the ionization states in the metal-nonmetal transition region and the corresponding uncertainties can be remarkable. We believe that our hydrodynamic calculations of the sample thickness are not affected essentially by these uncertainties as long as the sample resides in this domain of the phase diagram during a sufficiently short period of time.

In Fig. 6 the dependencies of the relative volume versus specific enthalpy calculated by means of the two EOS models[21,22] are compared with the experimental data.[13,25] As one can see, the SESAME model shows a large discrepancy in the relative volume of liquid aluminum compared to the measured data. The model[22] has turned to be more accurate in describing the liquid aluminum thermodynamics. Comparison of both EOS models in the gaseous state region with some other models found in the literature[10,11,26] is presented in Fig. 7. It should be noted that in the gaseous state region there are no reliable experimental data. As it follows from Fig. 7 both EOS models used in this work give very similar results in this region.

For the hydrodynamic calculations of the sample thickness we need also an EOS model for the surrounding medium confining the sample, i.e., for silica glass and sapphire. The following semiempirical EOS model describing uniaxial adiabatic flow generated in the medium was utilized:

$$P = \frac{B}{n}\left[\left(\frac{\rho}{\rho_{02}}\right)^n - 1\right], \tag{5}$$

where the coefficient B and the exponent n are assumed to be constant. These constants are related by an equation with the longitudinal sound speed c_2 and the density ρ_{02} of the material at standard conditions. The coefficients B and n were found by fitting of the literature data on the mechanical properties of the materials[27–29] and are listed in Table I.

IV. MHD CALCULATIONS OF THE SAMPLE THICKNESS

Numerical simulation in the framework of the complete 1D MHD model[17,18] was performed to choose the parameters of our experiments, which ensure sufficiently homogeneous heating. All experiments were done for the parameters of choice. In the case of homogeneous heating the calculations of the sample thickness [to obtain the conductivity according to Eq. (4)] can be essentially simplified in comparison to those performed using the complete MHD model. In particular, these calculations can be done for prescribed temporal dependencies of the Joule heating power and the electrical current through the sample (which can be taken in this case from the corresponding experiment). In doing so one should solve instead of the complete system of the MHD equations only the hydrodynamic part of the equations (expressing the laws of conservation of mass, linear momentum, and energy), the right-hand parts of which are some given functions of time (see Ref. 17 for details). Thus, there is no need for a conductivity model in these calculations. The system of equations in this case takes the form

$$\frac{\partial \rho}{\partial t} + \frac{\partial(\rho u)}{\partial x} = 0, \tag{6}$$

$$\frac{\partial(\rho u)}{\partial t} + \frac{\partial}{\partial x}(\rho u^2 + P) = -\frac{4\pi}{c^2} j(t)^2 x, \tag{7}$$

$$\frac{\partial}{\partial t}\left(\rho\varepsilon + \frac{\rho u^2}{2}\right) + \frac{\partial}{\partial x}\left[\rho u\left(w + \frac{u^2}{2}\right)\right] = \rho\frac{dq(t)}{dt}, \tag{8}$$

where ρ, u, P, and ε are density, velocity, pressure, and specific internal energy, respectively, w is the specific enthalpy,

TABLE I. Parameters of the EOS (5) used in the hydrodynamic calculations.

	ρ_{02} (g/cm^3)	B (GPa)	n
Silica glass	2.2	50	0.6
Sapphire	3.98	499	2.8

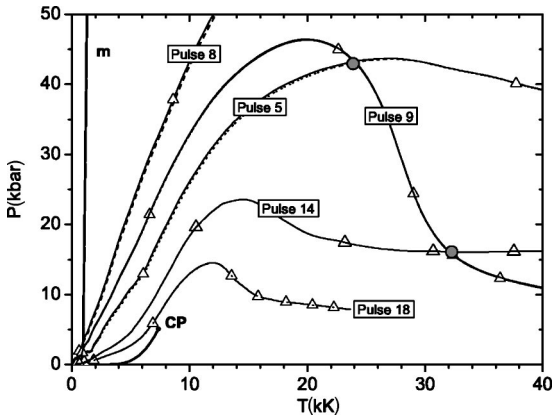

FIG. 8. Evolution of the thermodynamic state of aluminum foil strips confined in glass (pulses 14 and 18) and sapphire plates (pulses 5, 8, and 9) during the pulse Joule heating calculated by means of the 1D hydrodynamic code using the EOS model of Ref. 22. Thermodynamic paths of the two fixed particles of the sample (in the sense of the continuous media mechanics) for each experiment are presented: a particle situated close to the specimen surface (dashed line) and a particle near the symmetry plane (solid line); for pulses 9, 14, and 18 both lines nearly coincide. The melting line (m), and the boiling curve with a critical point (CP) are also shown. The open triangles indicate the time marks in 0.25-μs intervals. Gray circles mark two states reached by different paths.

which is related to the internal energy by $w=\varepsilon+P/\rho$, and c is the speed of light in vacuum. All the variables are functions of the position x and the time t (see Fig. 1). The electrical current density j is expressed through the total current $I(t)$ by

$$j(t)=\frac{I(t)}{hd(t)}. \tag{9}$$

Since the effects of heat conduction, viscosity, and heat transport by radiation are insignificant, the corresponding terms do not enter the equations of motion (6)–(8).

The equations of motion for the confining medium have the same form (6)–(8), but in this case the right-hand parts are equal to zero, i.e., it is assumed that the medium is a good insulator. The interface between the sample and the glass is treated like a contact surface. It should be noted that in the case of an inhomogeneous heating such an approach can no longer be applied and a conductivity model is needed.

The paths in the (P,T) plane of several heating processes realized in our experiments with aluminum foil strips tamped by glass and sapphire plates are presented in Fig. 8. The paths were calculated using the above-mentioned approach, i.e., for the prescribed temporal dependencies of the Joule heating power and the current. Each of the experiments shown in this figure is illustrated by two trajectories representing two thin layers in the sample: a surface layer (dashed line) and a layer near the symmetry plane (solid line). These two layers correspond to two cells from the 50–100 cells in the sample region of the spatial mesh used in these simulations. As follows from Fig. 8, variations of the temperature and pressure across the sample did not exceed 5%. Such nonuniformities are developed mainly due to the pinch effect and the effect of inertia when the heating power changes rapidly. To relate the path for pulse 5 to the temporal dependencies shown in Fig. 4 the time marks in the 250 ns interval are indicated.

A series of experiments was carried out in this study to be certain that the sample is heated homogeneously. In particular, experiments with different sample widths and thickness and different confining media (silica glass and sapphire) were carried out. None of these parameters appeared to have a remarkable influence on the electrical conductivity results. Many of our experiments were repeated (at least two times) to get the information about the uncertainty of the measured quantities. It was determined that the current and voltage are measured with an uncertainty less than 5%. The resistance as a function of the Joule heat released for different pulses with all parameters kept constant shows a scatter of less than 10%.

To demonstrate that the complete procedure of determination of the resistivity is self-consistent (when some quantities are measured and other are calculated), several experiments were performed, in which a thermodynamic state [say, in the (P,T) plane] is achieved by substantially different paths. The gray circles in Fig. 8 mark two such states. Experiment 9 was carried out using relatively thin sapphire plates (1.5 mm) so that the rarefaction wave reflected from the free surface reaches the sample in a shorter time in comparison to experiments 5 and 14. The heating current pulse was taken in this case so that the sample thickness is still rather small so the homogeneous state of the sample is not disturbed essentially by the rarefaction wave. As a result it was found that the values of the resistivity determined for these two states in different experiments are within the experimental uncertainty of 10–20 %. This can be clearly seen in Fig. 9.

V. ELECTRICAL RESISTIVITY OF ALUMINUM IN LIQUID AND GASEOUS STATES

The results obtained on the resistivity of hot aluminum in the metal-nonmetal transition region for 13 pulses are presented in Fig. 9. The dashed lines represent the dependencies of the resistivity versus temperature for 8 experiments. The corresponding lines for the remaining 5 experiments were dropped to avoid image oversaturation because those experiments repeat some of the experiments presented in Fig. 9. The dynamic pressure generated in all 13 experiments was remarkably higher than the critical pressure. Both the temperature and the sample thickness were calculated in this case using the EOS model from Ref. 22. As one can see, the lines representing experiments 9 and 5 intersect at a temperature of about 23 500 K, which agrees well with the calculations of the temperature at the point where the corresponding thermodynamic paths intersect (see Fig. 8). The dependencies of the resistivity on temperature for experiments 14 and 9 also have an intersection point but it is located at a substantially higher resistivity value (of about 34 $\mu\Omega$ m, and the temperature at that point is about 30 000 K), which is out of the scope of Fig. 9. The gray circles show the resistivity values corresponding to four fixed relative volumes: $V/V_0=1.93$, 2.7, 4.0, and 5.4; the data along isochores represent

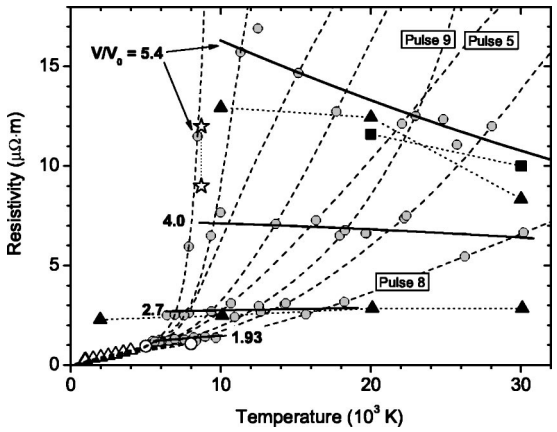

FIG. 9. Resistivity of aluminum vs temperature in the metal-nonmetal transition region. The dashed lines represent our experiments. The gray circles correspond to present data at the isochores $V/V_0=1.93$, 2.7, 4, and 5.4. The solid lines are fits of our data at these isochores. The other designations are measurements by Gathers (Ref. 13) (open triangles), calculations by Silvestrelli (Ref. 9) at $V/V_0=1.93$ (open circles), calculations by Desjarlais *et al.* (Ref. 12) at $V/V_0=2.7$ and 5.4 (solid triangles), calculations by Kuhlbrodt and Redmer (Ref. 7) at $V/V_0=5.4$ (solid squares), the measurements by Mostovych and Chan (Ref. 4) (open stars). For purpose of clarity the data points of Refs. 4, 7, and 12 are connected by dotted lines.

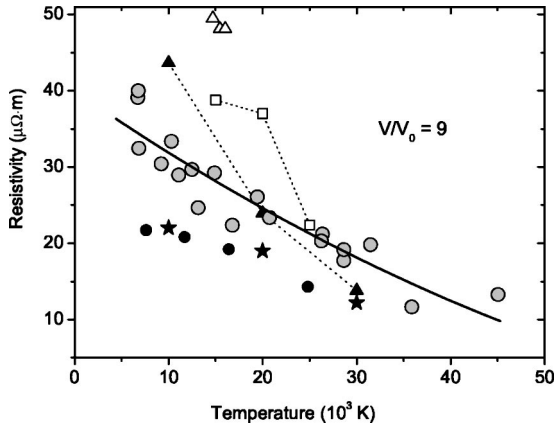

FIG. 10. Resistivity of dense aluminum plasma vs temperature at constant density ($V/V_0=9$). The gray circles represent our data, the thick solid line is a parabolic fit of our data points, measurements by Renaudin *et al.* (Ref. 10) (open triangles), measurements by Krish and Kunze (Ref. 14) (open squares), calculation results of Ref. 10 (solid stars), calculations by Kuhlbrodt and Redmer (Ref. 7) (solid squares), calculations by Desjarlais *et al.* (Ref. 12) (solid triangles).

all 13 experiments to show scattering of our data. Solid lines are fits of these data sets. The points along isochores $V/V_0=1.93$ and 2.7 were fitted by straight lines, and the points at $V/V_0=4.0$ and 5.4 were fitted by parabolas. Left points for $V/V_0=4.0$ and 5.4 were not included in the data sets for the fitting. These points show a new tendency in the resistivity behavior at the lower temperatures ($T<12\,000$ K). The fitting curves clearly demonstrate a change in the temperature dependence of the resistivity in the metal-nonmetal transition region. The measurement results by Gathers[13] are also presented in this figure (open triangles). As it can be seen in Fig. 9, the results from Ref. 13 are very close to present data at $T\leqslant 4000$ K. Our measurements at the low temperatures agree well also with the calculations fulfilled by Silvestrelli[9] for liquid aluminum at the relative volume of 1.93.

It is obvious that the resistivity values along the isochore $V/V_0=2.7$ are in excellent agreement with the calculation results from Ref. 12, which demonstrate practically a constant resistivity value over the whole temperature range investigated in this work. For $V/V_0=5.4$ reasonable agreement also takes place with the results obtained in Ref. 7. Nevertheless, in contrast to the theoretical predictions our results demonstrate a maximum in the temperature dependence of the resistivity along this isochore. At this isochore (and even at $V/V_0=4.0$) the temperature derivative of the resistivity (at $T>12\,000$ K) becomes negative, manifesting a transition of aluminum in a dielectric state.

The dependencies of the resistivity on temperature for relative volumes $V/V_0=9$ and 27 are presented in Figs. 10 and 11. Published experimental results[10,11,14,15] along with the theoretical predictions[7,10–12] are also shown for comparison. A considerable discrepancy for $V/V_0=9$ takes place between present results and the measurement results presented in Refs. 10 and 15. However, for both these isochores our data are in good agreement with those of Ref. 14. Comparison of our data with the calculated dependence presented in Ref. 12 shows good agreement in the case $V/V_0=9$. For $V/V_0=27$ our measurements give resistivity values that are remarkably higher than those predicted in all theoretical works.[7,10–12] It is obvious that our results demonstrate the best agreement with the finite-temperature density-functional calculations results.[9,12]

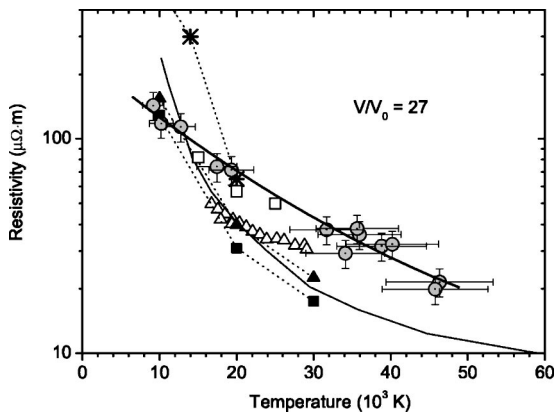

FIG. 11. Resistivity of dense aluminum plasma vs temperature at constant density ($V/V_0=27$). The gray circles represent our data and the thick solid line is a parabolic fit of our data points (error bars are shown for present experiments), measurements by DeSilva and Katsouros (Ref. 15) (stars), measurements by Krisch and Kunze (Ref. 14) (open squares), measurement results by Renaudin *et al.* (Ref. 10) (open triangles), calculation results of Ref. 10 (thin solid line), calculations by Desjarlais *et al.* (Ref. 12) (solid triangles), calculations by Kuhlbrodt and Redmer (Ref. 7) (solid squares).

VI. DISCUSSION

The present results show a remarkable discrepancy with respect to the measurement results obtained in Ref. 10. Those measurements were performed with aluminum foils confined in a high-pressure vessel to provide an isochoric heating. The foils were heated by a current pulse of rather low density (during 300 to 700 μs). Due to a relatively large ratio of the vessel volume to the initial volume of the sample (9 and 27) the plasma was generated by vaporization of the foil at a pressure that is essentially lower than the critical pressure. As a result, an inhomogeneous two-phase liquid-vapor mixture filled the vessel at a vaporization stage of the heating process. The authors[10,11] assume that at later times the plasma becomes homogeneous. It can be clearly seen in Fig. 2 from Ref. 10 where the current and voltage traces are shown that the resistance of the sample monotonically increases during the experiment. The authors[10] have found that due to substantial energy losses (which take more than 50% of the total Joule heat imparted into the foil) the internal energy actually decreases despite the continuing heating. As a result, a plasmalike dependence of the resistivity of the sample was detected (a fall in the resistance with temperature), but only in a narrow temperature range from 14 500 to 16 000 K (see Fig. 10). Since the energy losses were proved to be so important, the sample mass could change remarkably due to the wall ablation effect. Therefore the cause of the discrepancy seen in Figs. 10 and 11 between our results and those reported in Ref. 10 can be explained by the wall ablation effect and the uncertainty in the internal energy calculation for a system that starts its evolution from an inhomogeneous state.

The measurement results presented by Krisch and Kunze[14] for three relative volumes (5.4, 9, and 27) are rather consistent with our data (within an experimental uncertainty of 20–25 % given in Ref. 14). To get the data points for the resistivity at the three isochores shown in Figs. 9–11 linear interpolations between the nearest-neighbor points presented in Ref. 14 were used. For the relative volumes of 5.4 and 9 the difference between our data and those of Ref. 14 is remarkably larger (especially at $T<20\,000$ K) than that for $V/V_0=27$. In Ref. 14 aluminum wires were placed in thick glass capillaries, one end of which was open. The plasma column diameter was measured by photographing the diameter of the plasma jet emanating from the open end of the capillary. The experimental uncertainty of such measurements was not determined in Ref. 14, but we assume that it can be considerable. Due to the uncertainty in the plasma density determination the discrepancy between our results and those of the work by Krisch and Kunze[14] is maximal in the density range where the dependence of the resistivity on density is strong. At the relative volume $V/V_0=27$ where this dependence becomes weaker the data obtained in Ref. 14 agree reasonably with present results.

The data presented in Ref. 15 were obtained using the exploding wire technique with water as a confining medium. Those data agree with our results well only for $V/V_0=27$ when $T\geqslant 20\,000$ K. At smaller volumes and temperatures there is an essential difference. The data points from that work for the relative volumes of 5.4 and 9 are out of the scope of Figs. 9 and 10. For instance, the resistivity values from Ref. 15 for $V/V_0=5.4$ are two times larger than present data. Our simulations show that this discrepancy is caused mainly by inhomogeneous heating of the plasma generated in experiments by DeSilva and Katsouros.[15] The maximum inhomogeneity is developed when the plasma column diameter is 2–4 times larger than the initial wire diameter. At larger diameters the temperature and density profiles become fairly uniform due to some features in the hydrodynamic flow generated in those experiments.

Now we pass to comparison of our data with theoretical predictions. Molecular dynamics simulations based on the finite-temperature density-functional approach were performed by Silvestrelli.[9] The simulations were done to investigate the temperature and density dependencies of the electrical conductivity of liquid aluminum, whose density is 30–50 % lower than the normal solid density and the temperature is within the range of 3500 to 9000 K. At these temperatures and densities the reflectivity measurements of Ref. 4 indicated a sharp decrease in the conductivity. The simulation results[9] did not support the conclusions drawn in Ref. 4 about the onset of a metal-insulator transition in this density range. As it can be seen in Fig. 9, our results reasonably agree with those presented in Ref. 9. The maximal relative volume at which the calculations were done is $V/V_0=1.93$. At this volume the resistivity was calculated for two temperature values only: 5000 and 8000 K. It is interesting to note that even the slope in the dependence of the resistivity on temperature seen in our data is practically the same as predicted by Silvestrelli.[9] The data inferred from the reflectivity measurements are also shown in Fig. 9 for $V/V_0=1.93$. It is likely that the results of Ref. 4 suffer from a considerable error in the density evaluation.

An approach very similar to that of Ref. 9 was used by Desjarlais *et al.*,[12] where the calculations were done in a wide density range from near solid to one-hundredth solid density and in a temperature range from 2000 to 30 000 K. For the molecular dynamics runs, the ions and their respective core wave functions were modeled using the Vanderbilt ultrasoft pseudopotentials. The calculations were done for two isochores in the condensed state region ($V/V_0=1.35$ and 2.7) and for three isotherms (10 000, 20 000, and 30 000 K) in the gaseous state region. Our measurement results demonstrate a reasonable agreement with those of the calculations[12] for $V/V_0=2.7$. It should be noted that the last point on the left in Fig. 9 from Ref. 12 for $V/V_0=2.7$ corresponds to a thermodynamic state of expanded aluminum located deeply inside the two-phase region ($T=2000$ K). The estimates of the critical temperature of aluminum give the values ranging from 6000 to 8000 K.[5,23]

To investigate the resistivity behavior at lower pressures (to reach the lowest temperature point of Ref. 12 for $V/V_0=2.7$) several experiments were done with wires and foils submersed in water. In this case the dynamic pressure was in the range of 2–4 kbar. The resistivity values obtained in these experiments turned out to be remarkably higher than those obtained in our experiments with glass and sapphire plates. For instance, for $V/V_0=2.7$ instead of the resistivity value of 3 $\mu\Omega$ m we obtained a value of about 5 $\mu\Omega$ m. 1D MHD simulations performed for these experimental condi-

tions have shown that such a resistivity increase can be rather accurately described by the volume vaporization (boiling) model,[16] which neglects by the vaporization kinetics effects (effects of overheating). The boiling kinetics effects were proved to be in the case of tungsten not significant up to the heating times of the order of 1 ns.[30] It was assumed in the hydrodynamic simulations that the substance in the two-phase region is a fine dispersed mixture, which can be treated as an effective medium. As result of the simulations it was concluded that in our experiments the one-phase states close to the left point of Ref. 12 for $V/V_0=2.7$ cannot be achieved. Probably it will be possible to reach the superheated states (without onset of boiling) when aluminum samples of very high purity are used.

Our data show a nonmonotonic behavior of the resistivity versus temperature for $V/V_0=5.4$ (and even for $V/V_0=4$). Desjarlais *et al.*[12] discuss a gap in the electronic density of states, which begins to form near the Fermi level at $V/V_0=5.4$. This is the possible reason for the change in the slope of the resistivity on temperature dependence for this isochore. The calculation results[12] in the gaseous state region ($V/V_0=9$) also show a rather consistent behavior of the resistivity compared to that seen in our data. Nevertheless our results demonstrate two new features in the resistivity behavior: the clearly expressed negative slope in the resistivity on temperature dependence at $V/V_0=4.0$, and the maximum along the isochore $V/V_0=5.4$.

A very difficult question is how to estimate the accuracy of present data because not all quantities were measured and we utilize the EOS model, whose accuracy is unknown over the whole temperature and density range investigated. We have compared the resistivity values obtained using the two EOS models.[21,22] As a result it was found that in the gaseous state region ($V/V_0>6$) the difference between these resistivities is less than 20%. Taking into account this value as an uncertainty and the experimental uncertainties in the current, voltage, and the sample dimensions measurements the error bars shown in Fig. 11 were obtained.

Before finishing the discussion we present some estimates showing that the features discovered in this study can be interpreted based on the metal-nonmetal transition concept. First, it is interesting to note that at a relative volume $V/V_0=2.3$ the mean free path Λ_e of the valence electrons (conducting electrons) becomes equal to the interionic separation d_{ii}. Therefore at the larger expansions ($V/V_0>2.3$) the Ioffe-Regel condition, that is, $\Lambda_e \geqslant d_{ii}$, is violated. To calculate the mean free path we used the experimental values of the conductivity assuming the following formula is valid:

$$\sigma = \frac{n_e e^2 \Lambda_e}{m v_F}, \tag{10}$$

where n_e is the valence electron number density, e is the electron charge, m is the electron mass, and v_F is the Fermi velocity. The electron number density is related to the ionic number density n_i by $n_e=zn_i$, where z is the number of the conducting electrons per ion (z was taken to be 3). The interion spacing d_{ii} was calculated according to the relationship

$$\frac{\pi}{6} d_{ii}^3 n_i = 0.63. \tag{11}$$

This relation expresses a condition that the hard sphere packing fraction in the liquid state is equal to 0.63 as in the case of dense random packing. Based on such estimates of the mean free path one can conclude that at the larger expansions, i.e., at $V/V_0>2.3$ the abrupt resistivity increase observed in our experiments is due to a decrease in the valence electron number density rather than in the mean free path (because it has reached its minimal value, $\Lambda_e \approx d_{ii}$). Therefore the point of localization also represents the limit of characterizing the aluminum as a free-electron metal, which has been pointed out by Silvestrelli.[9]

Another estimate supporting this conclusion can be done using the Clausius-Mossotti relationship:

$$\varepsilon = \frac{1+\frac{8\pi}{3}\alpha n_i}{1-\frac{4\pi}{3}\alpha n_i}, \tag{12}$$

where ε is the dielectric constant and α is the atomic polarizability. The metal-nonmetal transition in a compressed aluminum vapor occurs when the dielectric constant diverges. The corresponding value of the relative volume calculated is 3.3. We used for the atomic polarizability of aluminum atom a value $\alpha=56.28a_0^3$ from Ref. 19 (a_0 is the Bohr radius). At this relative volume the transition from a dielectric to a metallic state occurs in an aluminum vapor when it is pressurized at a sufficiently low temperature. This value agrees well with the present experimental result, which demonstrates a dielectriclike behavior in the temperature dependence of the resistivity at the relative volume value of 4 and a metalliclike behavior at $V/V_0=2.7$.

VII. CONCLUSIONS

We have found that a sharp increase in the temperature dependence of the resistivity of expanded liquid aluminum takes place at a density of about 1.3 g/cm^3 ($V/V_0 \approx 2$) when the pressure is in a range of 7–20 kbar. When the pressure approaches a value of about 20 kbar the sharp resistivity increase disappears and the temperature dependence of the resistivity is like that in the solid state region. Along the isochore $V/V_0=2.7$ the resistivity is practically constant over the whole temperature range investigated in present study (6000–20 000 K). A dielectriclike dependence of the resistivity on temperature is observed at a density that is 4 times less than the normal solid density. At a temperature of about 12 000 K for an isochore $V/V_0=5.4$ a maximum in the temperature dependence of the resistivity was detected.

It is interesting to note that practically all measurements (except of that of Ref. 10) give very close conductivity values for $V/V_0=27$. At this density a typical discrepancy between the measurement results and theoretical predictions is 50–100 %.

The present results are in essential agreement with those of the molecular dynamics simulations based on finite-temperature density-functional theory.[9,12]

ACKNOWLEDGMENTS

We thank Dr. S. E. Rosenthal for assistance in getting SESAME EOS data and Scott Crockett for delivering table 3720. We are indebted to Dr. M. P. Desjarlais for sending us the data set of the results published in Ref. 12. We also thank Dr. Jens Haun, who kindly provided us with the dissertation of Dr. Ingo Krisch. This work was performed under the financial support of Presidium of Russian Academy of Sciences in the framework of the program on "Thermophysics and mechanics of intense energetic influences."

*Electronic address: savlab@iht.mpei.ac.ru

[1] I. K. Kikoin and A. P. Senchenkov, Fiz. Met. Metalloved. **24**, 843 (1967).
[2] Ya. B. Zel'dovich and L. D. Landau, Zh. Eksp. Teor. Fiz. **14**, 32 (1944).
[3] F. Hensel, Philos. Trans. R. Soc. London, Ser. A **356**, 97 (1998).
[4] A. N. Mostovych and Y. Chan, Phys. Rev. Lett. **79**, 5094 (1997).
[5] V. E. Fortov and I. T. Yakubov, *Physics of Non-ideal Plasmas*, 1st ed. (World Scientific, Singapore, 2000), Vol. 1, p. 14.
[6] A. W. DeSilva and H.-J. Kunze, Phys. Rev. E **49**, 4448 (1994).
[7] S. Kuhlbrodt and R. Redmer, J. Phys. A **36**, 6027 (2003).
[8] J. F. Benage, W. R. Shanahan, and M. S. Murillo, Phys. Rev. Lett. **83**, 2953 (1999).
[9] Pier Luidgi Silvestrelli, Phys. Rev. B **60**, 16 382 (1999).
[10] P. Renaudin, C. Blancard, G. Faussurier, and P. Noiret, Phys. Rev. Lett. **88**, 215001 (2002).
[11] P. Renaudin, C. Blancard, J. Cle'rouin, G. Faussurier, P. Noiret, and V. Recoules, Phys. Rev. Lett. **91**, 075002 (2003).
[12] M. P. Desjarlais, J. D. Kress, and L. A. Collins, Phys. Rev. E **66**, 025401(R) (2002).
[13] G. R. Gathers, Int. J. Thermophys. **4**, 209 (1983).
[14] I. Krisch and H.-J. Kunze, Phys. Rev. E **58**, 6557 (1998).
[15] A. W. DeSilva and J. D. Katsouros, Phys. Rev. E **57**, 5945 (1998); Int. J. Thermophys. **20**, 1267 (1999).
[16] A. D. Rakhel, A. Kloss, and H. Hess, Int. J. Thermophys. **23**, 1369 (2002).
[17] V. N. Korobenko, A. D. Rakhel, A. I. Savvatimskiy, and V. E. Fortov, Plasma Phys. Rep. **28**, 1008 (2002).
[18] A. D. Rakhel, V. N. Korobenko, A. I. Savvatimskiy, and V. E. Fortov, Int. J. Thermophys. **25**, 1203 (2004).
[19] *CRC Handbook of Chemistry and Physics*, edited by D. R. Lide and H. P. R. Frederikse (CRC Press, London, 1993–1994).
[20] G. I. Kanel, S. V. Rasorenov, and V. E. Fortov, in *Shock Compression of Condensed Matter—1991*, edited by S. C. Schmidt, R. D. Dick, J. W. Forbes, and D. G. Tasker (Elsevier Science, New York, 1992), p.451.
[21] Scott Crockett, Los Alamos National Laboratory Report No. LA-UR 04-6442, 2003 (unpublished); Los Alamos National Laboratory Report No. LA-UR 92-3407, 1992, edited by S. P. Lyon and J. D. Johnson (unpublished).
[22] A. D. Rakhel, Report on the Session of the Scientific Council on Physics of Low-Temperature Plasma of the Russian Academy of Sciences, Moscow, November 1999 (unpublished).
[23] D. A. Young, Lawrence Livermore Laboratory Report No. UCRL-52352 (1977) (unpublished).
[24] M. M. Basko, Teplofiz. Vys. Temp. **23**, 483 (1985).
[25] V. V. Ivanov, S. V. Lebedev, and A. I. Savvatimskii, J. Phys. F: Met. Phys. **14**, 1641 (1984).
[26] G. Kresse and J. Hafner, Phys. Rev. B **47**, R558 (1993).
[27] L. M. Barker and R. E. Hollenbach, J. Appl. Phys. **41**, 4208 (1970).
[28] R. A. Graham and W. P. Brooks, J. Phys. Chem. Solids **32**, 2311 (1971).
[29] H. Sugiura, K. Kondo, and A. Sawaoka, J. Appl. Phys. **52**, 3375 (1981).
[30] A. D. Rakhel and G. S. Sarkisov, Int. J. Thermophys. **25**, 1215 (2004).